Korean J. Chem. Eng., **29**(6), 731-736 (2012)
DOI: 10.1007/s11814-011-0241-z

Structural and photoelectrochemical characterization of TiO_2 nanowire/nanotube electrodes by electrochemical etching

Jing Ya†, Li An, Zhifeng Liu, Lei E, Wei Zhao, Dan Zhao, and Chengcheng Liu

Department of Materials Science and Engineering, Tianjin Institute of Urban Construction, Tianjin 300384, China
(*Received 5 May 2011 • accepted 9 September 2011*)

Abstract–TiO_2 nanowire/nanotube electrodes were synthesized by anodization of titanium foils in ethylene glycol solution containing 0.5 wt% NH_4F and 1 wt% water at 60 V for 6 h. The microstructure and morphology of the as-prepared electrodes were investigated by XRD and SEM. A possible formation mechanism and oxidation parameters of nanocomposite structure were discussed. The relationship between structural characteristics of TiO_2 nanowire/nanotube electrodes and its photoelectrochemical characterization were evaluated by electrochemical analyzer and photocatalytic degradation of methylene blue (MB) solution. Furthermore, these TiO_2 nanowire/nanotube electrodes promoted the photoelectrochemical characterization due to the larger surface areas, enhanced light harvesting and electron transport rate. The results show that photocurrent density of 1.44 mA/cm^2 and photocatalytic degradation of 95.51% was achieved for TiO_2 nanowire/nanotube electrodes, which were 0.55 mA/cm^2 and 20.52% higher than the TiO_2 nanotube electrodes under a similar condition, respectively.

Key words: TiO_2 Nanotube Electrodes, Nanowires, Electrochemical Anodization, Photocatalytic Activity, Electrochemical Etching

INTRODUCTION

Titanium dioxide (TiO_2) is known to be one of the best catalysts due to its unique structure, remarkable properties and wide-range potential applications in photocatalysis, photoelectrocatalysis, photovoltaic cells, water splitting, degradation of organic pollutants biocompatible materials [1-3]. Over the past several years, TiO_2 nanostructures have become the focus of considerable interest due to their unique properties [4]. Owing to the superior photoelectrochemical, mechanical and biocompatible properties, TiO_2 nanowires [5], nanosheets [6], nanorods [7] and nanotubes [8-10] have been widely studied for many different applications. An important feature of all these electrode architectures is the vectorial electron transport pathway perpendicular to the charge collecting substrates, and the resulting generally superior electron collection, which is critical for high photoelectrochemical performance [11].

In recent years, increasing attention has been given to fabricating highly ordered TiO_2 nanotube electrodes, because it is expected that a remarkably enhanced photocatalytic activity can be achieved in comparison with other existing forms of TiO_2 [12]. This is closely related to the higher specific surface area and superior physical topology of nanotubes [13,14]. In addition, extensive investigations have been concentrated on the design and synthesis of nanocomposite oxides such as TiO_2 nanowire/nanotube electrodes; they could be prepared through a heterogeneous incorporation process [15]. The realization of bicomponent nanowires photocatalysts can achieve large surface exposure areas and improve the process of electron and hole transfer between the corresponding conduction and valence bands [16,17]. Therefore, such kinds of TiO_2 nanowire/nanotube electrodes have attracted much attention. However, the structural, optical and photoelectrochemical characterization of TiO_2 nanowire/nanotube electrodes by electrochemical etching has not been studied deeply.

In this study, TiO_2 nanowire/nanotube electrodes were synthesized by anodization of titanium foils in ethylene glycol solution containing 0.5 wt% NH_4F and 1 wt% water at 60 V for 6 h. The microstructure and morphology of the as-prepared electrodes were investigated by XRD and SEM. A possible formation mechanism and oxidation parameters of nanocomposite structure were discussed. The relationship between structural characteristics of TiO_2 nanowire/nanotube electrodes and its photoelectrochemical characterization were evaluated by electrochemical analyzer and photocatalytic degradation of MB solution. We envision that these TiO_2 nanowire/nanotube electrodes promote the photoelectrochemical characterization due to the larger surface areas, enhanced light harvesting and electron transport rate.

EXPERIMENTAL

1. Preparation of TiO_2 Electrodes

The chemicals were of analytical grade and used without further purification. All the solutions were prepared with distilled water. The titanium foils (0.5 mm thick, 99.6% purity, from Tianjin Gerui, China) with a size of 10 mm×20 mm were used as starting materials. Prior to any electrochemical treatment, the titanium foil was mechanically polished with different abrasive papers and cleaned in an ultrasonic bath containing cold distilled water for 15 min, then chemically etched in strong acidic mixture solution of HF and HNO_3 (HF : HNO_3 : H_2O=1 : 4 : 5 in volume) for 30 s to form a fresh smooth surface. The last step of pretreatment was rinsing the solution with acetone, absolute alcohol and distilled water in turn. The substrate

†To whom correspondence should be addressed.
E-mail: yajing_tj@126.com

was then dried in air at room temperature. Anodization was performed in a two-electrode configuration with one titanium foil as the working electrode and the other foil with the same area as the counter electrode under constant potential at room temperature. The interval between working electrode and counter electrode was about 3 cm. TiO_2 electrodes were formed in an electrolyte comprised of 0.5 wt% NH_4F and 1-5 wt% H_2O in ethylene glycol at constant potential supplied by a DC power (YJ32-1, Shanghai). The as-prepared electrodes were immersed into absolute alcohol bath overnight and ultrasonically cleaned in absolute alcohol for 30 s to remove any surface debris, then dried in air naturally. Finally, to crystallize the TiO_2 electrodes, obtained in amorphous form by anodic growth, the sample was placed in a tubular furnace for 2 h at 450 °C with a slope of 2 °C/min in air, so to be transformed into the anatase phase, which shows higher photoelectrochemical properties.

2. Characterization

A field emission scanning electron microscope (FESEM; Hitachi, S-4700) is used to analyze the morphology of TiO_2 electrodes. X-ray diffraction (XRD) patterns of the as-prepared electrodes were performed using a diffractometer (Model D/max 2,500 V, Rigaku Co., Japan, Cu K_α. λ=0.15406 nm determine the crystal phase and size.

All electrochemical measurements were performed on a TD3691 electrochemical analyzer (TD Co., Tianjin) with a conventional three-electrode system comprised of platinum foil as an auxiliary electrode, saturated calomel electrode (SCE) as reference, and TiO_2 electrodes as a working electrode. A 1 mol/L Na_2S solution was chosen as the supporting electrolyte in the experiment. A concentration of 1 mol/L is able to provide adequate electrical conductivity to minimize the high resistance of narrow channel between the anodic and cathodic compartment in the reactor. All the regions, except a 1 cm^2 area, were covered with an insulating epoxy. A 250 W high pressure mercury lamp (Beijing Huiyixin, China) was used as the simulated solar light with central wavelength of 365 nm as a UV light source, and the light source was away from the working electrode with a distance of 10 cm; all experiments were performed at room temperature.

A set of photocatalytic degradation experiments were done in the following procedure: The as-prepared electrodes with an area of 4 cm^2 were placed in 20 mL of MB solution, which has an initial concentration of 10 mg/L. Prior to the photoreaction, the electrode was placed in the reactor and left there for about 30 min to achieve the adsorption/desorption equilibrium in the dark environment; then the reaction was irradiated at room temperature by the UV light (8 W, CBIO, 254 nm) from the top vertically. During the photoreaction, the reaction solution was analyzed by UV-Vis spectrophotometer (7230G, Shanghai) at different times. The analytical wavelength selected for optical absorbance measurement was 660 nm.

RESULTS AND DISCUSSION

Fig. 1 illustrates the current transient curve recorded during the anodization of titanium foil in ethylene glycol solution containing 0.5 wt% NH_4F and 1 wt% water at 60 V for 6 h. It can be clearly seen that anodization in electrolyte leads to changes in the mode of current, showing a decrease/increase/decrease sequence, but the values of current densities are signicantly different; most important,

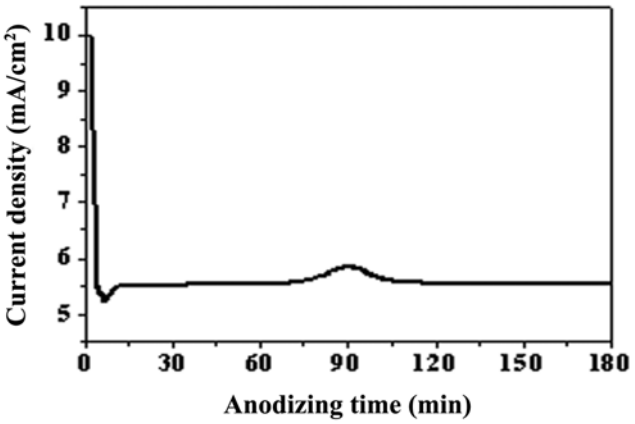

Fig. 1. Current density-anodization time curve for electrochemical anodization.

the growth rates of TiO_2 electrode differ greatly. In the early stages of the process, the rapid decrease of the current density is due to a non-conductive thin oxide layer, which is formed on the surface of the titanium foil. In the next stage, before reaching a quasi-steady state value, a slight increase in the current density appears, due to the local growth of the pores. This constant current is due to an equilibrium between a continuous dissolution of titanium dioxide according to the following reaction and the oxidation of metallic titanium. According to the theory proposed by Grimes et al. [18-21], the formation of the TiO_2 nanowire/nanotube electrodes happens in this part of the anodization because of the combined processes described in Eqs. (1) and (2):

$$Ti+2H_2O-4e^- \rightarrow TiO_2+4H^+ \quad (1)$$

$$TiO_2+6F^-+4H^+ \rightarrow [TiF_6]^{2-}+2H_2O \quad (2)$$

To elucidate the influence of some other key parameters on mor-

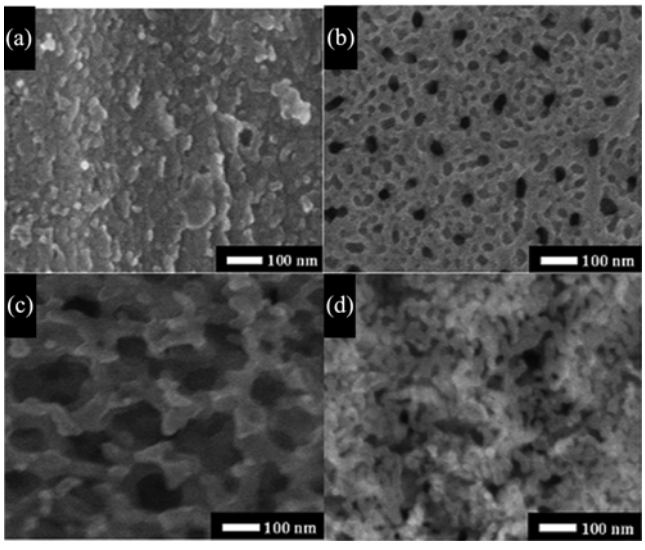

Fig. 2. SEM top-view images show the evolution of porous TiO_2 morphology after anodizing for (a) 5 min; (b) 60 min; (c) 90 min; (d) 180 min in ethylene glycol solution containing 0.5 wt% NH_4F and 1 wt% water at 60 V.

phology and dimension, a set of experiments were performed under the different conditions. Fig. 2 indicates the evolution of the morphology of the porous TiO_2 in ethylene glycol solution containing 0.5 wt% NH_4F and 1 wt% water for various anodizing times at 60 V. Fig. 2(a) shows the SEM micrograph, which was obtained within 5 min of voltage supply. It confirms that the drastic drop in current density is attributable to the oxidation of the Ti foil to form TiO_2 layer However, with the time of anodization increased to 60 min, few small pits originated in the oxide layer could be observed in Fig. 2(b). Beyond this point, the current density also increased to reach a maximum value of 6 mA/cm^2. The increase in current density is caused by the formation of pits and enlargement of the pits on the oxide layer as shown in Fig. 2(c). And then current density drops slowly, probably due to the competition between the growth and dissolution of the oxide layer to form a stable nanotube. This is because Ti-hydroxide precipitate is formed via the instantaneous hydrolysis reaction, which leads to the generation and the accumulation of Ti-hydroxide precipitate at the top of nanotubes as shown in Fig. 2(d) [22].

Microstructure characterization of anodic TiO_2 electrodes has been carried out for morphological analysis. Fig. 3(a) and 3(b), (c) are the scanning electron microscopy (SEM) images of the surface and the profile view of the TiO_2 nanotube electrodes, respectively. The nanotubes oxide layer was formed by anodization in ethylene glycol solution containing 0.5 wt% NH_4F and 5 wt% water at 30 V for 8 h. The pH of the electrolyte was adjusted at 4.5 by a small amount of phosphoric acid during the entire process. The nanotubular were ordered and vertically oriented. The vertical growth of oxide nanotubes from the iron substrate was expected to give the least resistance to electron transport. TiO_2 nanotube electrodes show an inside diameter of 100-110 nm and a wall thickness of 10-15 nm and that the tube length is approximately 7.7 μm. Fig. 3(d) and 3(e), (f) show SEM images of TiO_2 nanowire/nanotube electrodes which are obtained from ethylene glycol with 0.5 wt% NH_4F and 1 wt% water for 6 h at 60 V. As is observed, the obtained TiO_2 nanowire/nanotube electrodes had an interconnected composite structure. The top surface of the freestanding TiO_2 nanotube electrodes was covered with a layer of TiO_2 nanowires. Herein, the surface thin layer is composed of dense TiO_2 nanowires with an average width of 40-50 nm, which is also the same as a film thickness of approximately 200 nm.

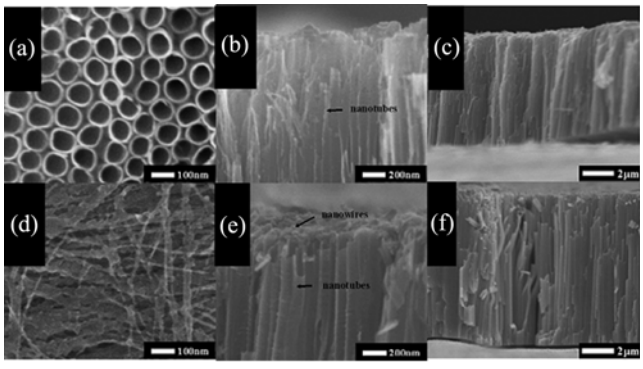

Fig. 3. SEM images of the TiO_2 electrodes (a) top view of TiO_2 nanotube electrodes; (b), (c) profile view of TiO_2 nanotube electrodes; (d) top view of TiO_2 nanowire/nanotube electrodes; (e), (f) profile view of TiO_2 nanowire/nanotube electrodes.

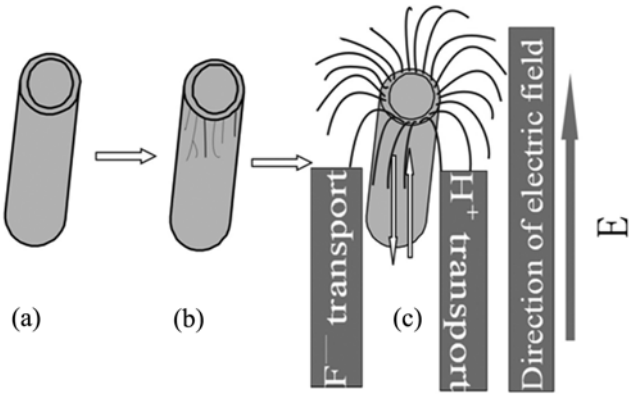

Fig. 4. Schematic diagram of the mechanism of the formation of nanowires on anodic TiO_2 nanotube electrodes. (a) growth of nanotubes; (b) splitting of the nanotubes by electric-field-directed chemical etching; (c) formation of nanowires by further splitting; E: the direction of electric field.

It is also observed from Fig. 3(d) that the underlying layer is the highly ordered TiO_2 nanotube electrodes with the pore size of about 120-130 nm and wall thickness of 20 nm. TiO_2 nanotube electrodes are one-dimensional, compact (nanotubes were well attached to each other) and vertically oriented (straight). Such a nanocomposite structure film is composited of the compact packing nanowires and the highly ordered nanotubes with length of 11.5 μm.

Fig. 4, the schematic diagram of formation mechanism of TiO_2 nanowires through longitudinally splitting off nanotubes at pore mouth was proposed. The anodization allows for the preparation of TiO_2 nanotube electrodes, which are vertically split off by electric-field-directed electrochemical etching [21,23-25]. According to Misra et al., a small amount of water is essential for the formation of anodic TiO_2 nanotube electrodes [26]. In the case of less water content, the electrolysis of water mainly takes place at the pore bottom of nanotubes due to its maximum electric field, leading to a local low pH value. This condition provides a favorable environment for the growth of nanotubes at the tip by fluorine ions. The viscous ethylene glycol solution allows a localization of this low pH condition at the pore bottom, thereby restricting the chemical dissolution of nanotubes at the pore mouth. In addition, if a high potential is employed, the hydrogen ions generated on the surface of nanotubes are consequentially driven to the cathode by the electric field, leading to the creation of an interface tension stress of nanotubes in the viscous electrolyte. Chemical dissolution of TiO_2 nanotube electrodes may occur along with this stress; thereafter, a longitudinal flow of ions in the channel of nanotubes caused by a high electric field is responsible for vertically splitting off nanotubes in the viscous electrolyte and producing the nanowires. Since water electrolysis in ethylene glycol medium is an inefficient reaction, the chemical etching process is suppressed and the longitudinal splitting reaction of nanotubes is also restrained at the pore mouth. Accordingly, this leads to the formation of TiO_2 nanowires on the entire TiO_2 nanotube electrodes. The mechanism of the nanowires formation is described based on the bamboo-splitting model.

Fig. 5 shows the X-ray diffraction (XRD) patterns of TiO_2 electrodes annealing at a temperature of 450 °C for 2 h in air, which can cause a complete phase of transferring from amorphous structure

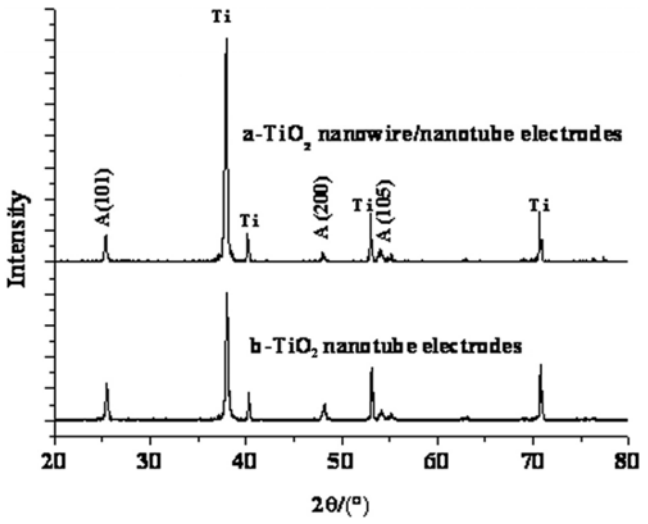

Fig. 5. XRD patterns of TiO_2 electrodes.

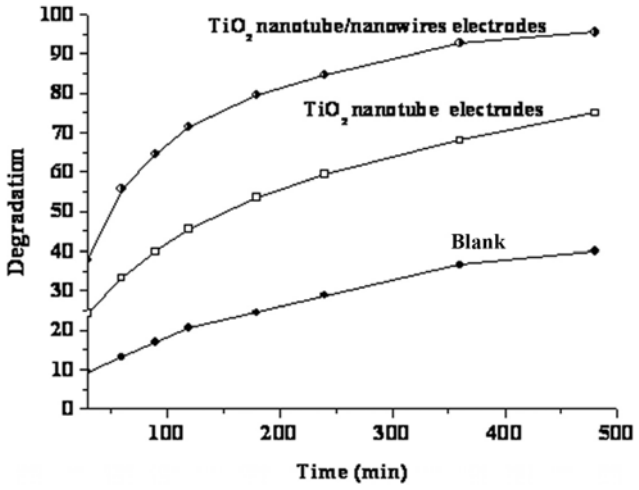

Fig. 7. Comparison of photocatalysis efficiency of TiO_2 electrodes.

to anatase structure. The crystallinity of TiO_2 electrodes is quantitatively evaluated via the relative intensity of the (101) diffraction peak of the anatase and exhibits typical diffraction peaks of metallic titanium. These values closely match those reported in anatase phase of TiO_2 (JCPDS card no. 21-1272). The typical diffraction peak of TiO_2 nanotubes is more intensive than that of TiO_2 nanowire/nanotube electrodes, which is related to the total thickness of anodic TiO_2 electrodes.

Fig. 6 gives the photocurrent density which is generated by the TiO_2 nanotube electrodes and TiO_2 nanowire/nanotube electrodes in 1 mol/L Na_2S electrolyte under the illumination of a 250 W high pressure mercury lamp. With the applied potential increased, the photocurrent increases linearly and reaches the maximum at 0.6 V (vs SCE). However, a saturation of the photocurrent was observed for the TiO_2 electrodes with potential ranging from 0 to 0.6 V; it is revealed that the transportation and creation of photo-electrons arrive at a steady state. The photocurrent density of the TiO_2 nanowire/nanotube electrodes at a bias potential of 0.6 V (vs SCE) is about

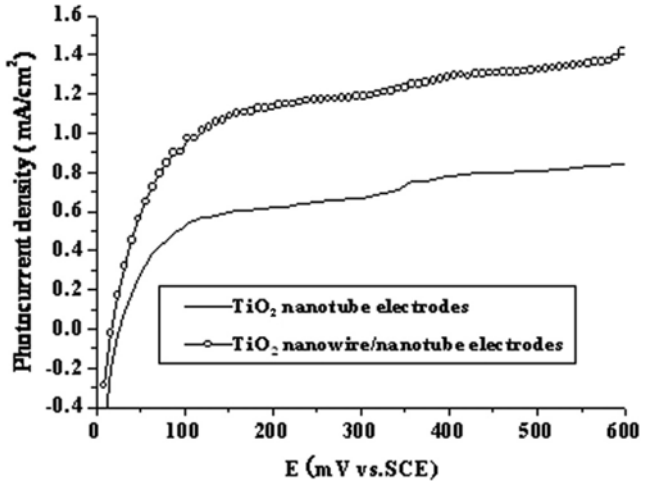

Fig. 6. Photocurrent density of TiO_2 electrodes.

1.44 mA/cm^2, which shows high photoconductivity and the properties required for promising electrode materials. It should be noted this value was 0.55 mA/cm^2 higher than the value reported for TiO_2 nanotube electrodes under a similar bias condition. From these results it can be seen that the TiO_2 nanowire/nanotube electrodes with the nanowires top surface structure enjoy a more signicant advantage for charge transport than that without nanowire structure. The TiO_2 nanowires provided a direct approach to perfect alignment of TiO_2 nanotube electrodes, bringing about reasonably enhanced electron transport efficiency and expected widespread applications in relevant areas.

Photocatalytic activity of the TiO_2 electrodes is evaluated by photocatalytic degradation of MB solution at neutral pH. Fig. 7 is the observed degradation of MB vs. illumination time catalyzed with different electrodes. The curves are the adsorption spectrum of the MB solution at different photodegradation periods. A blank test curve with no photocatalyst being employed is also given for comparison. The blank test confirms that MB solution is only slightly degraded under intensively visible light in absence of catalyst, while photocatalyzed tests show obvious impact on the decomposition profiles. The photocatalytic degradation of MB solution shows a different scenario. In the initial stage, the TiO_2 nanowire/nanotube electrodes with the nanowires top surface structure have excellent absorption characteristics than the TiO_2 nanotube electrodes. It also been observed that the saturated adsorptive capacity of TiO_2 nanowire/nanotube electrodes was 37.86% and TiO_2 nanotube electrodes 24.27%. This is ascribed to the larger contact area between TiO_2 nanowire/nanotube electrodes and solutions as evaluated from the SEM images. However, as the experiment went on, TiO_2 nanowire/nanotube electrodes still had relatively high rates of photodegradation. This is because TiO_2 nanowire/nanotube electrode allows rapid electron transfer from nanowires to nanotubes, which hinders recombination. In this survey, the photocatalytic degradation ratio achieves 95.51% for TiO_2 nanowire/nanotube electrodes, which is 20.52% higher than TiO_2 nanotube electrodes alone. TiO_2 nanowire/nanotube electrodes with the nanowires top surface structure had better photocatalytic activity, which is consistent with the report of the photocurrent density.

The structural characteristics of TiO_2 nanowire/nanotube elec-

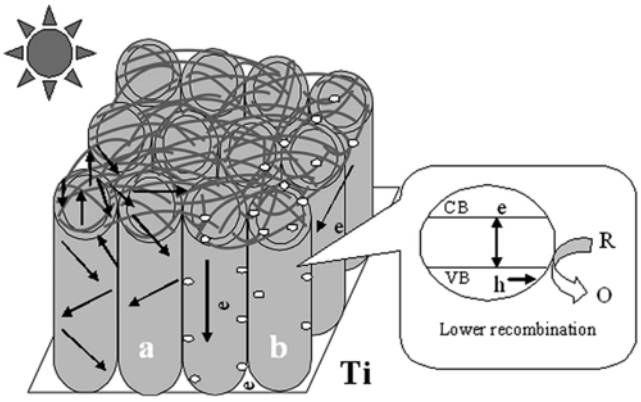

Fig. 8. Structural characteristics of TiO_2 nanowire/nanotube electrodes.

trodes is demonstrated in Fig. 8; compositing the disordered nanowires on the top surface and highly ordered nanotubes on the underlying layer, has been fabricated by longitudinally splitting off nanotubes in a controlled anodization process. Noticeably, such kinds of TiO_2 nanowire/nanotube electrodes can effectively promote the photoreactivity due to the larger surface areas, the enhanced light harvesting and electron transport rate [27,28]. The advantages of the proposed composite nanostructures are as follows: as is shown in Fig. 8(a), highly well-oriented TiO_2 nanowires entangled with each other to form a macroporous structure. This result elaborates on two important issues. First, the conguration of the TiO_2 nanowire/nanotube electrodes with the nanowires top surface structure allows the diffusion of reactants through multiple pathways to enhance light harvest. Second, the composite structure has a large surface exposure area to the surroundings, and the hetero-junction structure can promote the charge separation of the photogenerated electrons and holes within the composite nanostructures so as to enhance photocatalytic reaction [29-33]. Schematically illustrated in Fig. 8(b) is a possible electron transport pathway across the nanowire/nanotube electrodes to the conductive titanium substrate. Although such an electron transport pathway is in a zigzag fashion compared with well-aligned nanotubes, the nanowire/nanotube electrodes should still exhibit better charge transport, because the characteristic symmetrically branched structure of the nanowire/nanotube electrodes ensures that at least one of its nanowires roughly points to the direction to the nanotubes. Therefore, the resulting composite nanostructures may have high quantum efficiency and lead to high photocatalytic activity.

CONCLUSIONS

TiO_2 nanowire/nanotube electrodes were synthesized by anodization of titanium foils in ethylene glycol solution containing 0.5 wt% NH_4F and 1 wt% water at 60 V for 6 h. Like bamboo splitting, the nanowires originate from longitudinally splitting off nanotubes at the pore mouth. Compared with the TiO_2 nanowire/nanotube electrodes and TiO_2 nanotube electrodes, the composite structure electrode shows higher light harvesting efficiency and higher photovoltaic performance, which might contribute to their larger surface area, hollow interior wall and hierarchical porous structures. The results show that a photocurrent density of 1.44 mA/cm^2 and photocatalytic degradation of 95.51% was achieved for TiO_2 nanowire/nanotube electrodes, which were 0.55 mA/cm^2 and 20.52% higher than the TiO_2 nanotube electrodes under a similar condition, respectively.

ACKNOWLEDGEMENTS

This work was supported by Key Project in the Science & Technology Pillar Program of Tianjin (09JCYBJC02600) and National Natural Science Foundation of China (51102174).

RREFERENCES

1. K. S. Raja, V. K. Mahajan and M. Misra, *J. Power Sources*., **159**, 1258 (2006).
2. G. K. Mor, K. Shankar and M. Paulose, *Nano Lett*., **5**, 191 (2005).
3. D. W. Bahnemann, S. N. Kholuiskaya and R. Dillert, *Appl. Catal. B*., **32**, 161 (2002).
4. J. Kiss, L. Óvári and A. Oszkóa, *Surface Sci*., **605**, 1048 (2011).
5. J. B. Baxter and E. S. Aydil, *Sol. Energy Mater. Sol. Cells*, **90**, 607 (2006).
6. J. J. Qiu, Z. G. Jin and Z. F. Liu, *Thin Solid Films*, **515**, 2897 (2007).
7. E. Hosono, S. Fujihara and I. Honma, *Adv. Mater*., **17**, 2091 (2005).
8. J. M. Macák, H. Tsuchiya and A. Ghicov, *Electrochem. Commun*., **7**, 1133 (2005).
9. O. K. Varghese, D. W. Gong and M. Paulose, *Sens. Actuators, B*, **93**, 338 (2003).
10. S. S. Malwadkar, R. S. Gholap and S. V. Awate, *J. Photochem. Photobiol., A*, **203**, 24 (2009).
11. M. Paulose, G. K. Mor and O. K. Varghese, *J. Photochem. Photobiol., A*., **178**, 8 (2006).
12. V. Idakieva, Z. Y. Yuan and T. Tabakova, *Appl. Catal.,* A, **281**, 149 (2005).
13. L. V. Taveira, J. M. Macak and H. Tsuchiya, *J. Electrochem. Soc*., **152**, B405 (2005).
14. Y. H. Wang, H. X. Yang and H. M. Xu, *Mater. Lett*., **64**, 164 (2010).
15. X. Y. Pang, D. M. He and S. L. Luo, *Sens. Actuators, B*, **137**, 134 (2009).
16. C. Ruan, M. Paulose and O. K. Varghese, *J. Phys. Chem. B*, **109**, 15754 (2005).
17. M. Inoue and A. Murase, *Surf. Interface Anal*., **37**, 1111 (2005).
18. M. Paulose, K. Shankar and S. Yoriya, *J. Phys. Chem. B*, **110**, 16179 (2006).
19. C. A. Grimes, *J. Phys. Chem*., **15**, 1451 (2007).
20. N. K. Allam and C. A. Grimes, *Sol. Energy Mater. Sol. Cells*, **92**, 1468 (2008).
21. J. H. Lim and J. Choi, *Small*, **3**, 1504 (2007).
22. P. P. Das, S. K. Mohapatra and M. Misra, *J. Phys. D: Appl. Phys*., **41**, 245103 (2008).
23. Z. L. Xiao, C. Y. Han and U. Welp, *Nano Lett*., **2**, 1293 (2002).
24. D. Kim, A. Ghicov and P. Schmuki, *Electrochem. Commun*., **10**, 1835 (2008).
25. L. D. Sun, S. Zhang and X. W. Sun, *J. Electroanal. Chem*., **637**, 6 (2009).
26. J. Wang and Z. Q. Lin, *Chem. Mater*., **20**, 1257 (2008).
27. K. S. Raja, T. Gandhi and M. Misra, *Electrochem. Commun*., **9**, 1069

(2007).
28. W. Chen, H. F. Zhang and I. M. Hsing, *Electrochem. Commun.*, **11**, 1057 (2009).
29. Z. B. Wu, S. Guo and H. Q. Wang, *Electrochem. Commun.*, **11**, 1692 (2009).
30. J. S. Jang, H. G. Kim and Upendra A. Joshi, *Int. J. Hydrog. Energy*, **33**, 5975 (2008).
31. W. T. Yao, S. H. Yu and S. J. Liu, *J. Phys. Chem. B*, **110**, 11704 (2006).
32. Z. B. Wu, F. Dong and W. R. Zhao, *Nanotechnology*, **20**, 5701 (2009).
33. B. Lu, H. Li and L. Liao, *Nanotechnology*, **19**, 5605 (2008).